

# High-Temperature Superconductivity

Shoji TANAKA

*Superconductivity Research Laboratory/ISTEC, 1-10-13 Shinonome, Koto-ku, Tokyo 135-0062, Japan*

(Received July 27, 2006; accepted August 28, 2006; published online xxxx yy, zzzz)

A general review on high-temperature superconductivity was made. After prehistoric view and the process of discovery were stated, the special features of high-temperature superconductors were explained from the materials side and the physical properties side. The present status on applications of high-temperature superconductors were explained on superconducting tapes, electric power cables, magnets for maglev trains, electric motors, superconducting quantum interference device (SQUID) and single flux quantum (SFQ) devices and circuits. [DOI: 10.1143/JJAP.45.dummy]

**KEYWORDS:** BaPbBiO, LaBaCuO, YBaCuO, BiSrCaCuO, carrier concentration, two-dimensional CuO<sub>2</sub> structure, critical current, superconducting tape, bulk, Josephson effect, superconducting quantum interference device, single flux quantum device

## 1. Introduction

Superconductivity is a macroscopic quantum phenomenon; thus, its special physical properties have attracted the attention of many physicists and electric engineers, since it was discovered by Onnes in 1911. However, even though many types of superconductors were discovered for many years, the critical temperature was below 20 K, thus, the uses of superconductors required cooling using liquid helium.

After Nb<sub>3</sub>Ge ( $T_c = 23.2$  K) was discovered in 1973, the critical temperature did not increase by even 1 K for more than 10 years. Through the 1970s and 1980s, several types of experiments and theoretical discussions were carried out to discover “high-temperature superconductivity”. It is important to remember what happened in this prehistoric era.

Twenty years have passed since the first sample of high-temperature superconductivity was discovered in La<sub>2-x</sub>Ba<sub>x</sub>CuO<sub>4</sub> in 1986. Since then, many scientists rushed to these fields, and many types of high-temperature superconductors have been found in cuprate materials. A common fact in these materials is that quasi-two-dimensional superconductivity occurs in the vicinity of CuO<sub>2</sub> planes in the host materials, and the highest critical temperature at present is 135 K under atmospheric pressure in a mercury compound that was discovered in 1993.

As surprising characteristics of high-temperature superconductors have been revealed, on their research, application has accelerated in the last ten years. Developments include high-quality bulks, high-quality thin films and high-quality superconducting wires and tapes.

These will be used in electric communication systems, superconducting power cables, superconducting magnetic energy storage systems, electric motors and many other types of superconducting magnets.

Finally, it must be pointed out that further developments in new superconducting materials, having a higher critical temperature beyond 200 K, will occur. When a new breakthrough occurs, it will be very exciting.

## 2. Prehistoric View of High-Temperature Superconductivity

### 2.1 Situations in 1970s and 1980s

High-temperature superconductivity had been desired for many years by physicists and electric engineers. In particular, electric engineers hoped to use superconductors with a

critical temperature above liquid-nitrogen temperature, 77 K. However, after discovering the critical temperature of 23 K in Nb<sub>3</sub>Ge in 1973, the critical temperature was not raised by even 1 K. On the other hand, all of the superconducting phenomena could be explained by the elegant Bardeen–Cooper–Schrieffer (BCS) theory established in 1957.

The first famous prediction of high-temperature superconductivity was made by Frohlich in 1954,<sup>1)</sup> in which incommensurate charge density waves that occur by the Peierls transition in low-dimensional materials possibly move in the host lattice, and this may result in high-temperature superconductivity. However, even though charge density waves were observed in two-dimensional transition-metal dichalcogenides in 1970, and superconductivity was observed in NbS<sub>2</sub> and NbSe<sub>2</sub>, the critical temperatures were below 10 K.

In 1964, Little hypothesized that high-temperature superconductivity can be realized in one-dimensional structures on the basis of the exciton mechanism.<sup>2)</sup> According to his hypothesis, the system should contain long linear conducting molecules (polyenes or polymers with metallic atoms in an organic matrix), and on each side of these molecules groups of atoms with a high electronic polarizability should be located. These side branches should guarantee the mutual attraction of the conducting electrons as a result of the exchange of molecular excitations of the electronic type.

In 1977, Ginzburg and coworkers at the P. N. Lebedev Physical Institute in Moscow published a book entitled “High-Temperature Superconductivity”.<sup>3)</sup> In this book, they discussed the possibility of high-temperature superconductivity in many types of materials, including quasi-one and two-dimensional materials. The appearance of this book excited physicists in many countries.

In Japan, Nakajima coordinated a small group of theoretical physicists in 1982 and discussed the possibility of high-temperature superconductivity. In 1985, he expanded his group to include experimental physicists (the author was one of them) and started a new project entitled “New Superconducting Materials”, funded by the Ministry of Education in Japan.

In the United States, Geballe and coworkers organized an international workshop named “Mechanism and Materials of Superconductivity” in 1984, and the first meeting was held in Iowa.

In the late 1970s, new superconductors were discovered:

PbMo<sub>6</sub>S<sub>8</sub> by Chevrel and (SN)<sub>x</sub> by Hsu and Labes. However, the critical temperatures were low in both materials.<sup>4)</sup>

As discussed above, research on high-temperature superconductivity intensified worldwide in the 1970s and 1980s.

### 2.2 Oxide superconductors

In the 1960s, it was reported that SrTiO<sub>3</sub> becomes superconducting by oxygen doping, but that its critical temperature is low, approximately 1 K. In 1975, Sleight *et al.* found that BaPb<sub>1-x</sub>Bi<sub>x</sub>O<sub>3</sub> (BPBO) become superconducting when *x* is in the range of 0.1 to 0.3, and the highest critical temperature reaches 12 K.<sup>5)</sup>

By reading their short report, the author developed a strong interest in the research, and immediately started studying this material.<sup>6)</sup> Undoped BaPbO<sub>3</sub> has a perovskite structure and is insulating, and replacing some of the Pb with Bi results in doping of carriers due to the difference between the atomic values of the two elements. This method is usually employed in the field of semiconductors, and, by this method, much physical information can be obtained. In the case of BPBO, carrier concentration can be widely changed by doping; such a wide range change in the carrier concentration is impossible in ordinary metallic superconductors.

Then, the author and his coworkers measured the carrier concentrations in many samples by Hall-effect measurements and found the relationship between carrier concentration and critical temperature, as shown in Fig. 1. This result indicates that the critical temperature reaches 11.2 K at a carrier concentration of 10<sup>21</sup> cm<sup>-3</sup>, which is smaller than that of ordinary metallic superconductors by more than one order of magnitude.

The author named this material as a “low-carrier-concentration superconductor”. It is very important that even under such low carrier concentrations, the critical temperature can exceed beyond 10 K and that the superconductivity characteristics follow the BCS theory.

In the study of BPBO, we learned that insulating oxides can be conductors by “doping”, and in some cases become superconductors having a reasonable critical temperature. Furthermore, the bonding character of perovskite oxides is ionic rather than covalent, as in silicon; thus the constituent

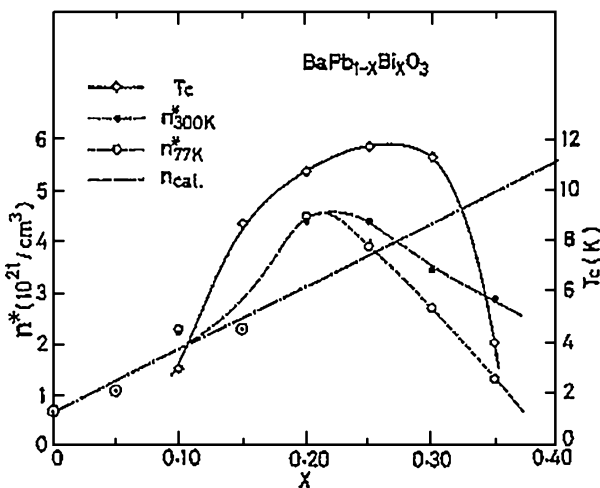


Fig. 1. Dependence of physical parameters on doping X.

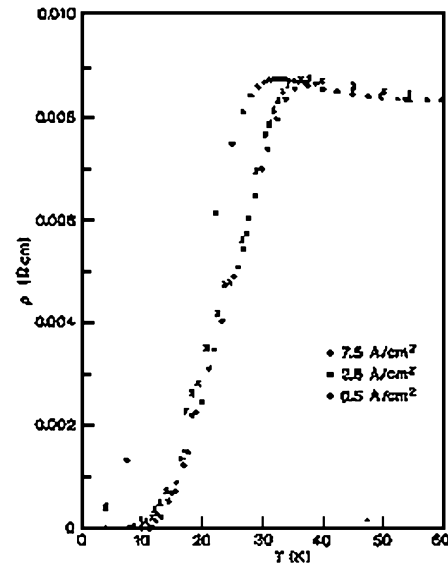


Fig. 2. Low-temperature resistivity of sample of Ba-La-Cu-O system for different current densities.

atoms can be replaced by a wide range of other types of atoms.

### 3. Discovery of High-Temperature Superconductivity in Cuprates

In 1986, following the study of BPBO, Bednorz and Muller tried a similar process using LaCuO<sub>3</sub>, and replaced some of the La by Ba, and found the possibility of high-temperature superconductivity.<sup>7)</sup> In a sample, they observed a rapid decrease in resistivity below 28 K, and at approximately 10 K, it becomes superconducting as shown in Fig. 2. Furthermore, they found that the resistivity curve against temperature shifts to the lower-temperature side with increasing electric current through the sample. They expected that this phenomenon resulted from the existence of high-temperature superconductivity.

Then, the author and his coworkers at the University of Tokyo began to search for true high-temperature superconductors. In December 1986, they found in La<sub>2-x</sub>Ba<sub>x</sub>CuO<sub>4</sub>, a) a sharp decrease in resistivity at 28 K, b) a clear increase in diamagnetic susceptibility, and c) a clear X-ray diffraction spectrum, which indicate that La<sub>2-x</sub>Ba<sub>x</sub>CuO<sub>4</sub> is a true high-temperature superconductor and its critical temperature is 28 K when *x* is nearly 0.15 (Fig. 3).<sup>8)</sup> Furthermore, from the magnetic susceptibility data, it was estimated that more than 30% of the material is superconducting, and this means that the material is real bulk superconductor. These results are the first confirmation of the existence of a high-temperature superconductor.

The crystal structure of La<sub>2</sub>CuO<sub>4</sub> is shown in Fig. 4, and its structure is two-dimensional. Thus, the author expected that the superconductivity in this material is two-dimensional,<sup>9)</sup> and this was proved later in many other experiments.

Soon after its discovery, it was shown that La<sub>2-x</sub>Sr<sub>x</sub>CuO<sub>4</sub> (LSCO) is also a high-temperature superconductor, having a higher critical temperature of 37 K. Since the crystal structure of this LSCO is the simplest one compared with those of other high-temperature superconductors found later,

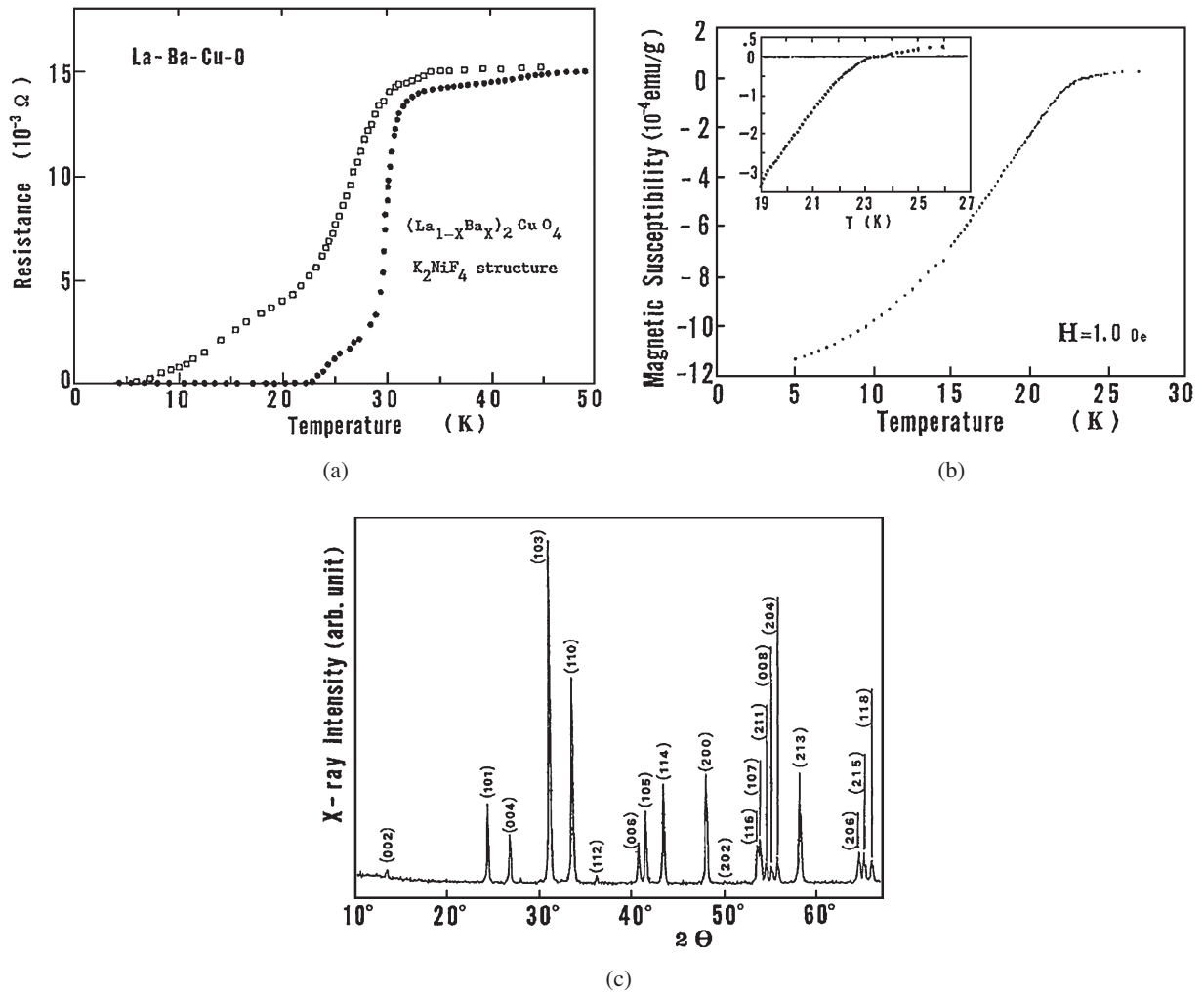


Fig. 3. Characteristics of  $\text{La}_{2-x}\text{Ba}_x\text{CuO}_4$ : (a) temperature dependence of resistivity and (b) magnetic susceptibility and (c) X-ray diffraction.

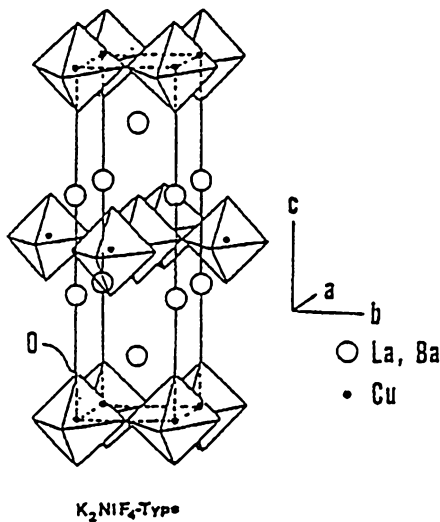


Fig. 4. Crystal structure of layered  $\text{La}_{2-x}\text{Ba}_x\text{CuO}_4$ .

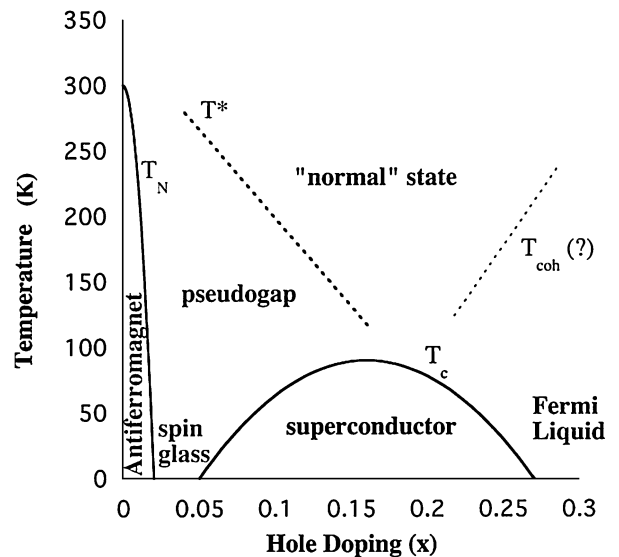


Fig. 5. Phase diagram of cuprates.

this material became the object of theoretical considerations. The phase diagram of LSCO is shown in Fig. 5, and shows that when  $x = 0$ , LSCO is antiferromagnetic and that its conductivity increases as  $x$  increases, and as  $x$  becomes larger, a superconducting phase appears, and then disappears

when  $x$  is larger than 25%. This diagram indicates that high-temperature superconductivity has a very complicated character. It must be mentioned that superconductivity occurs in the vicinity of the  $\text{CuO}_2$  layers in the host lattice.

It must be added that along the dashed line in the figure, a small phase transition is observed, which is called the "pseudogap state". The origin of this state is still not clear, and it might be a precursor of high-temperature superconductivity.

#### 4. A Wide Variety of So Many High-Temperature Superconductors

Since the first high-temperature superconductor was discovered in 1986, many scientists and engineers have searched for new materials, having a higher critical temperature. As a result, more than two hundred new materials were discovered, including many modifications of earlier materials. The reasons for such a large number of superconductors are a) the synthesis method is simple and does not require expensive apparatuses, and b) replacing one element with an other from the same group in the periodic table is strait forward.<sup>10)</sup> In Fig. 6, the crystal structures of representative high-temperature superconductors are shown. As mentioned before, a very common characteristic of these materials is that they are divided into two parts, CuO<sub>2</sub> planes

and blocking layers as shown in Fig. 7, and superconductivity occurs in only CuO<sub>2</sub> planes and the blocking layers supply charge carriers to the CuO<sub>2</sub> planes.

As new materials were rapidly discovered, the critical temperature rose sharply, as shown in Fig. 8. In this figure, only the names of materials that later became important for applications are given.

Generally, the control of oxygen content in oxide materials is very important. In the case of high-temperature superconductors, the behavior of oxygen is also important. The well-known YBa<sub>2</sub>Cu<sub>3</sub>O<sub>7</sub> (YBCO) has an orthorhombic structure (lattice constant along *a*-axis, *a* is different from *b*),

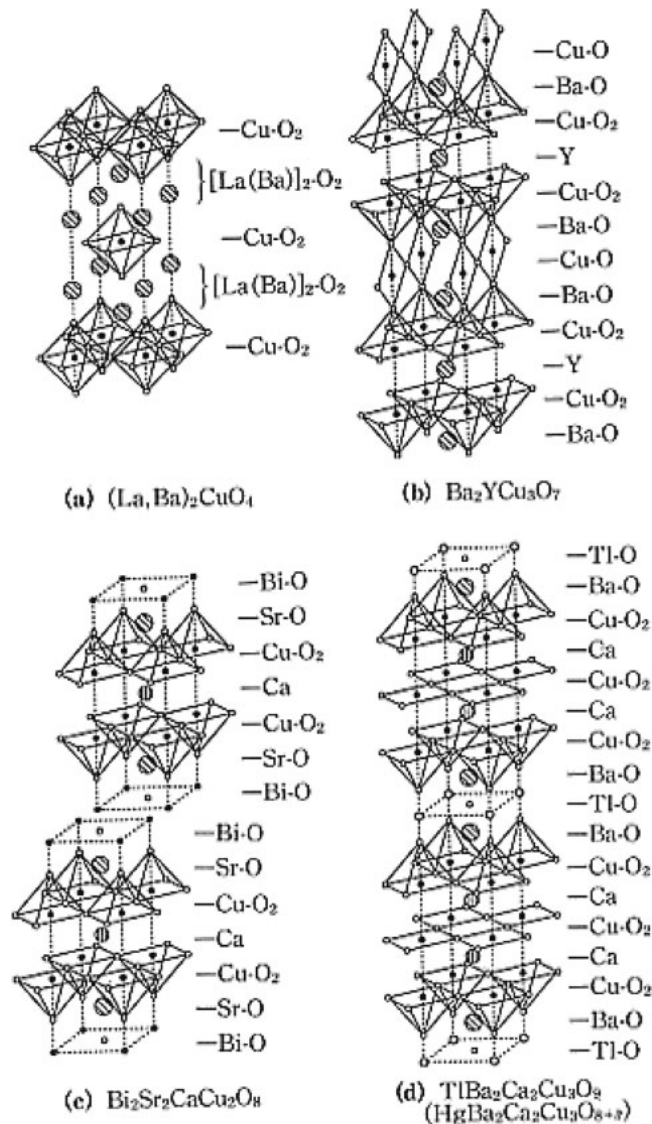


Fig. 6. Crystal structures of representative high-temperature superconductors.

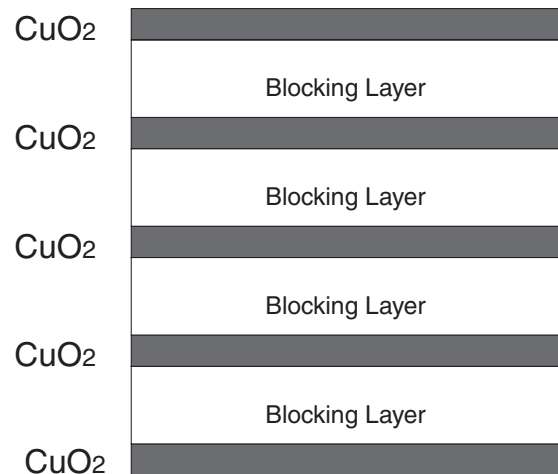


Fig. 7. Schematic structure of high-temperature superconductors.

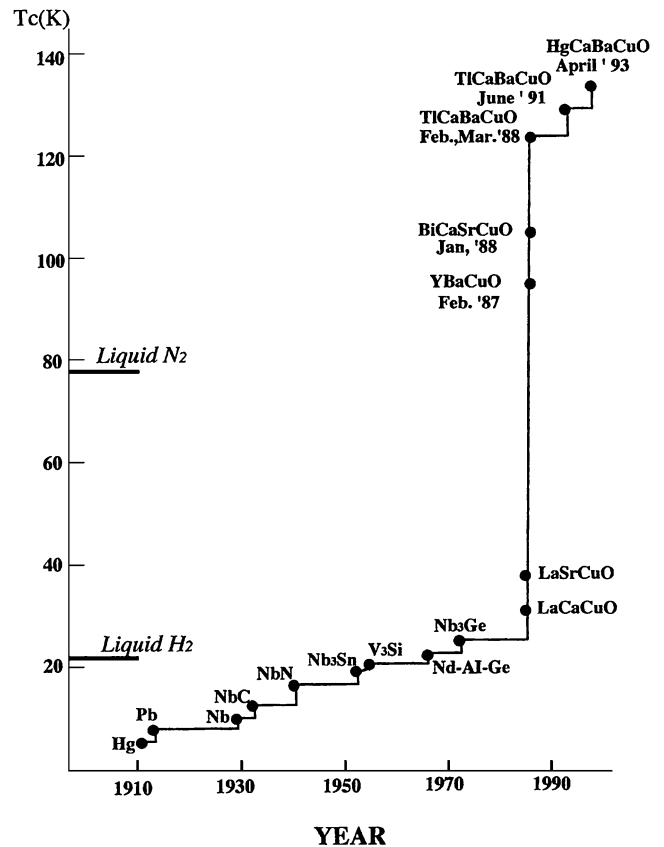


Fig. 8. History of high-temperature superconductors.

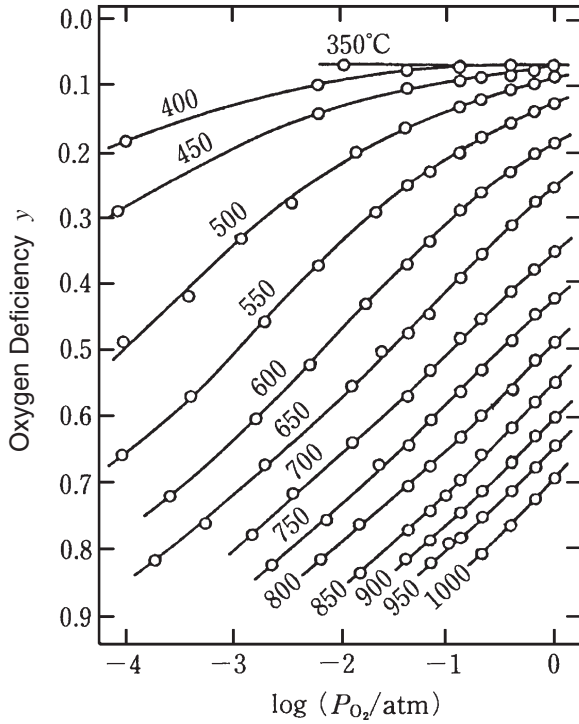


Fig. 9. Dependence of oxygen deficiency  $\gamma$  in  $\text{YBa}_2\text{Cu}_3\text{O}_{7-\delta}$ .

but it changes to tetragonal above 650 °C under a 100% oxygen atmosphere, as shown in Fig. 9,<sup>11)</sup> and the orthorhombic phase shows superconductivity at about 90 K. This is known as an “orthorhombic–tetragonal transformation”. These above-mentioned facts indicate that oxygen control is important in using high-temperature superconductors.

### 5. Specific Superconducting Characteristics

The characteristics of high-temperature superconductors are considerably different from those of ordinary low-temperature superconductors.

- The critical temperatures are higher by almost one order of magnitude.
- This means the superconductivity parameters  $\Delta^{(0)}$  are also larger by one order of magnitude.
- The penetration depths  $\lambda = (Me^*/\mu_0 n_s e^{*2})^{1/2}$  are much greater, because the carrier concentrations are much smaller by about two orders of magnitude.
- The coherent lengths of high-temperature supercon-

ductors  $\xi_0 = 2\hbar v_F/\pi\Delta^{(0)}$  are much smaller, and show strong anisotropy. In many cases,  $\xi_0$  perpendicular to the  $c$ -axis is 20 to 30 Å, but parallel to the  $c$ -axis,  $\xi$  is only a few Å. This indicates that the supercurrent along the  $c$ -axis occurs by Josephson coupling between  $\text{CuO}_2$  planes in many cases.

Thus, the Ginzburg–Landau (GL) parameter  $\kappa = \lambda/\xi$  is large, and the high-temperature superconductors are then said to be “extreme type II superconductors”.

- The superconductivity wave function has d-wave symmetry in high-temperature superconductors; on the other hand, that of low temperature superconductivity shows s-wave symmetry. This means that there are some points on the Fermi surface where the superconductivity gap disappears, as shown in Fig. 10. This characteristic becomes important when the critical-current problem is discussed later.

### 6. Magnetic Properties and Pinning Effects

The magnetic properties of high-temperature superconductors are very complicated, because quantized magnetic flux can penetrate the inside of materials, beyond the lower critical field  $H_{c1}$ . On the other hand, if the magnetic field reaches the upper critical field  $H_{c2}$ , the material is filled by normal cores and the superconductivity disappears. These two parameters are very important and are expressed by

$$H_{c1} = (\xi/\lambda)H_c \text{ and } \mu_0 H_{c2} = \Phi_0/\pi\xi^2.$$

Here,  $\Phi_0$  is the quantized flux and expressed by  $\Phi_0 = hc/2e$ , and then  $H_{c1}H_{c2} = H_c^2$ .  $H_{c1}H_{c2} = H_c^2$ , where  $H_c$  is the thermodynamic critical field. Since the GL parameter is very large in high-temperature superconductors, the upper critical field becomes a very high magnetic field. The region between  $H_{c1}$  and  $H_{c2}$  is known as the mixed state, where the normal state inside the core of the flux and the superconducting state coexist inside the material.

The motion of the magnetic flux is affected by the pinning effect. The flux is pinned by lattice defects, impurities and small particles of the normal state, and flux cannot move under the weak magnetic field, but if magnetic field becomes sufficiently strong, the flux becomes free from the pinning and can move with a loss of energy. The magnetic field, where the pinning effect is not effective, is called the “irreversible field”. These phases are shown in Fig. 11 schematically.

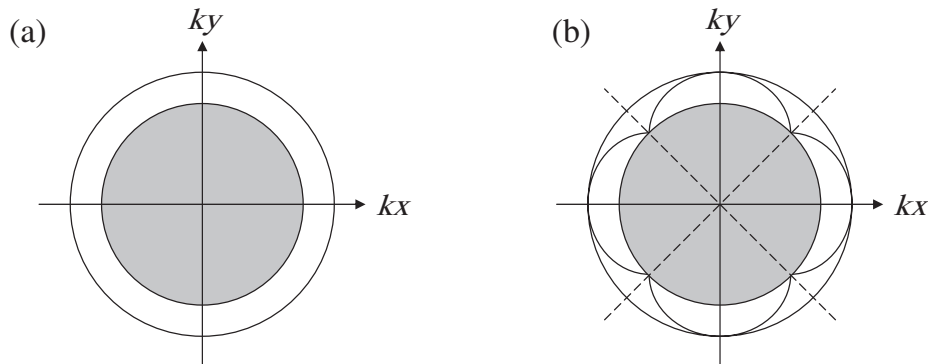


Fig. 10. Schematic representation of superconducting gap on Fermi surface: (a) s-wave and (b) d-wave symmetries.

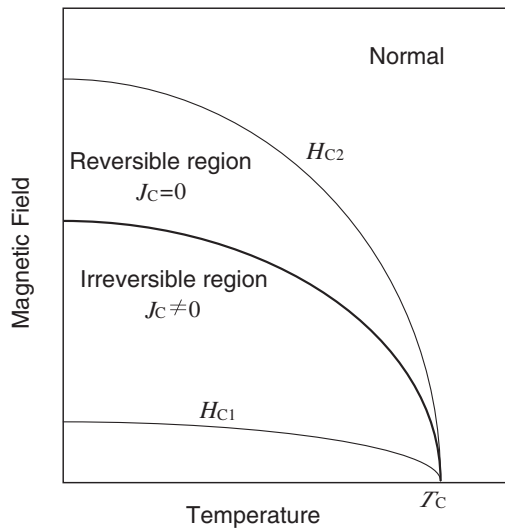


Fig. 11. Magnetic-phase diagram of high-temperature superconductors.

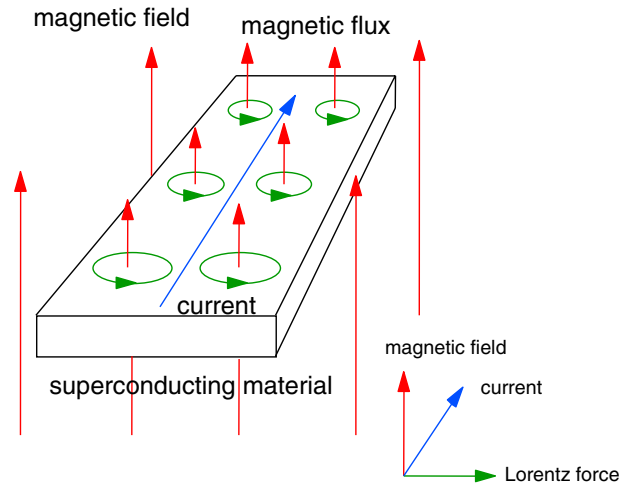


Fig. 13. (Color online) Magnetic flux inside sheet of high-temperature superconductors.

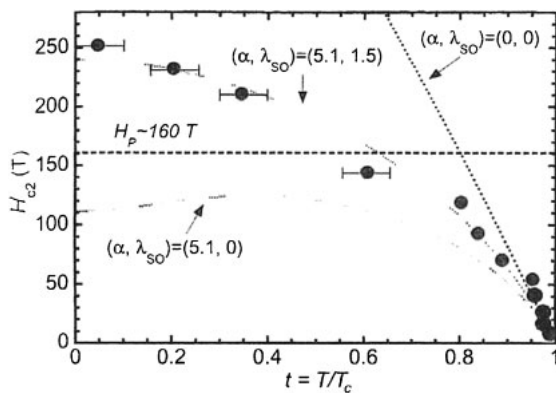


Fig. 12. Magnetic-phase diagram of upper critical field,  $H_{c2}$ (BiICuO<sub>2</sub>), for optimally doped YBCO.

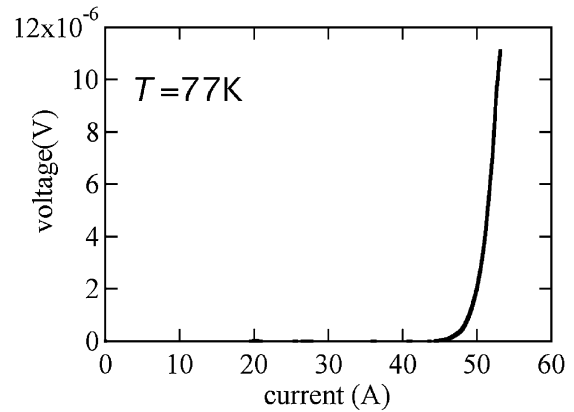


Fig. 14.  $I$ - $V$  Characteristics of YBCO film.

The  $H_{c2}$  of a single crystal of YBCO has been recently measured by Miura and his coworker by a pulsed magnetic field, and observed temperature dependences are shown in Fig. 12.<sup>12)</sup> These results show that  $H_{c2}$  becomes high, more than 100 T at low temperatures, which indicates that the irreversible field is more important in practical applications.

### 7. Critical-Current Problem

Figure 13 shows the case when the superconductor sheet is under a magnetic field perpendicular to the sheet. Then, the quantized magnetic flux is inside the sheet, as shown in the figure. When the super current flows in the sheet, flux moves in the direction of the Lorentz force with a loss of energy, and this means that resistivity appears inside the sheet. If such movements of flux are prevented by introducing suitable pinning centers, the resistivity becomes much smaller.

In Fig. 14, the super current dependence of the resistance (actually, the voltage between two terminals) of YBCO film is shown, and here the critical current is practically defined as the current at which the resistivity of the film becomes  $10^{-6}$  ohm/cm. The increase in resistance beyond the critical current depends on the quality of the film. In high-quality film, the increase is sharper.

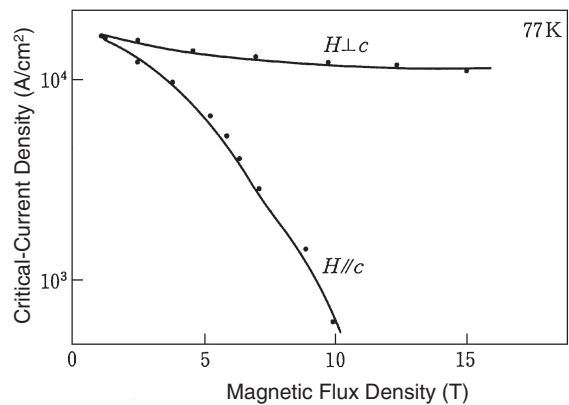
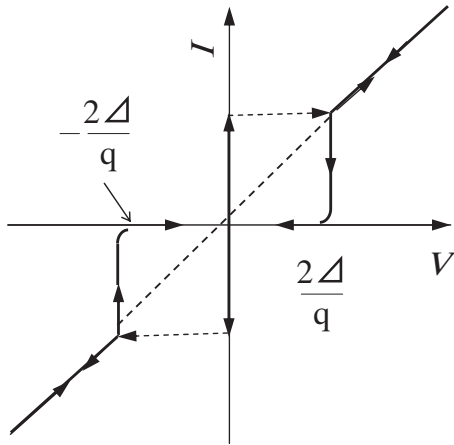


Fig. 15. Anisotropy of critical-current densities in YBCO bulk superconductor.

The critical-current density also shows strong anisotropy and this results from the difference between the structure of the magnetic flux and the structure of the pinning center along or parallel to the  $c$ -axis. As an example, the critical current densities in two cases in bulk YBCO at 77 K are shown in Fig. 15.<sup>13)</sup>

The critical-current problem is complicated and includes many factors other than the pinning problem, which will be discussed later.

Fig. 16.  $I$ - $V$  characteristics of S-I-S junction.

## 8. Josephson Effect

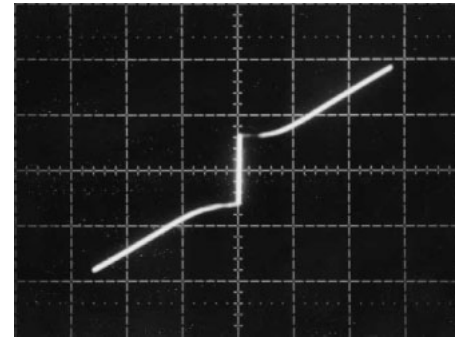
The Josephson effect is one of the most striking phenomena in the field of superconductivity. When two sheets of a superconductor are in contact through a very thin insulating layer, the tunneling of the Cooper pair occurs, and the current  $J$  is proportional to  $J_0 \sin \delta$ , where  $\delta$  is the difference between the phases of the superconducting wavefunctions on each side. This type of junction is known as an S-I-S junction and hysteresis appears in the current-voltage ( $I$ - $V$ ) characteristics, as shown in Fig. 16. On the other hand, when the thin layer is not insulating, the equivalent circuit of the junction is expressed as shown in Fig. 17(a) (resistance-shunted junction), and the  $I$ - $V$  characteristics do not show hysteresis, as shown in Fig. 17(b), and it is known as S-N-S junction.

In a Bi-2212 crystal with a highly two-dimensional structure, as shown in Fig. 7, the electric current parallel to the  $c$ -axis between adjacent  $\text{CuO}_2$  planes consists of Josephson coupling, and, in this case, the tunneling current characteristics follow those of the S-I-S junction. This type of tunneling is called an intrinsic Josephson junction.<sup>14)</sup>

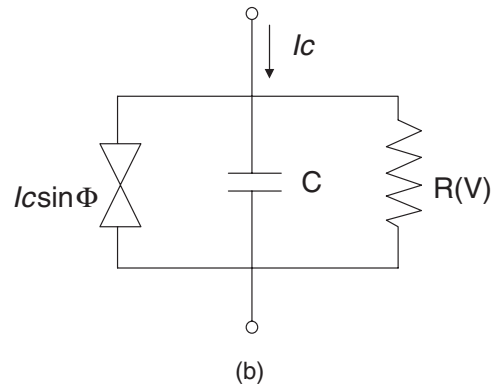
In the case of junctions of ordinary high-temperature superconductors such as YBCO, only S-N-S junctions can be fabricated, owing to the difficulty in fabricating an insulating layer between two superconductors, and typical  $I$ - $V$  characteristics of RSJ (resistively shunted junction) type are observed, as shown in Fig. 17. There are two types of Josephson junctions; one is a bicrystal type and the other is a ramp-edge type. The former is fabricated by sputtering superconducting film on the plate of a bicrystal of  $\text{SrTiO}_3$  and high-quality characteristics are obtained, which are used in high-sensitivity superconducting quantum interference device (SQUID) systems. In the ramp edge junction, the structure is complicated, as shown in Fig. 18, and this type of junction is mainly used in complicated circuits, as will be discussed later.

## 9. Applications of High-Temperature Superconductors

In the last 10 years, many applications of high-temperature superconductors have been developed. In this paper, some typical applications will be introduced.



(a)



(b)

Fig. 17. Equivalent circuit and  $I$ - $V$  characteristics of S-N-S junction.

### 9.1 Superconducting bulk and its applications

Superconducting bulk YBCO is grown using half-melt materials at a high temperature of nearly  $1000^\circ\text{C}$ , followed by a very slow cooling. The bulk almost has a single-crystal-like structure, and a large critical current of more than  $10^5 \text{ A/cm}^2$  is obtained at liquid-nitrogen temperature.

The special feature of the bulk is that the introduction of pinning centers is easily carried out by controlling the density of fine  $\text{Y}_2\text{BaCuO}_5$  particles as pinning centers in the bulk. The most distinguishing characteristic is that it is possible to trap a strong magnetic field of 2 to 3 T, even at liquid-nitrogen temperature. This value is much higher than the magnetic field of an ordinary permanent magnet.

Recently, the mechanical strength of bulk has been increased by polymer impregnation, and this bulk has trapped a very high magnetic field of 17 T at 30 K.

Superconducting bulk has been applied as a bearing system that is used to store electricity in a flywheel system, as shown in Fig. 19. The capacity of this system is about 10 kW/h and it has operated safely for many months.

The second application is a magnetic separation system for the water cleaning made by Hitachi, Ltd. The impurity particles in water join magnetic particles, and they are removed from the filter by the strong magnetic field of the bulk. The operation can be continuous and results have been impressive.

### 9.2 Superconducting tapes

#### 9.2.1 Silver-sheathed tape with Bi-2223 superconductor

At present, this type of superconducting tape is only commercially available in Japan by Sumitomo Electric Industries, Ltd. As is shown in Fig. 20, the tape is 4 mm

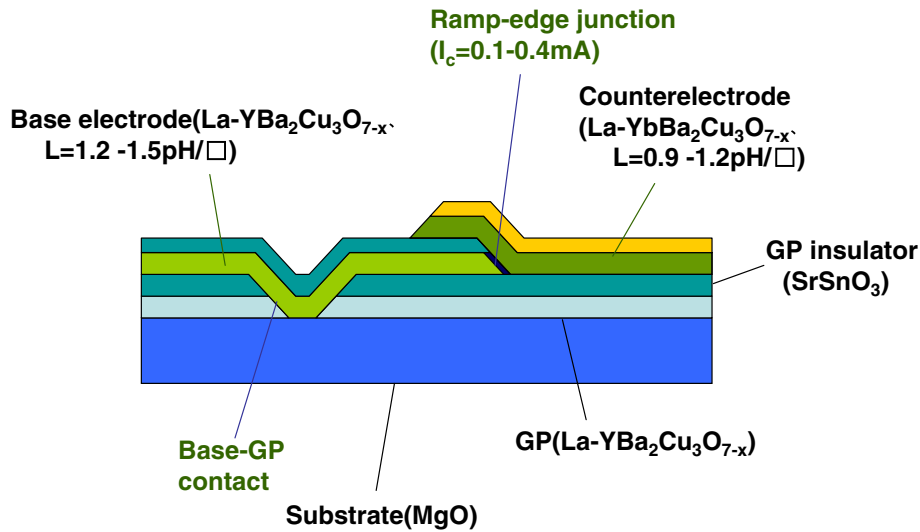
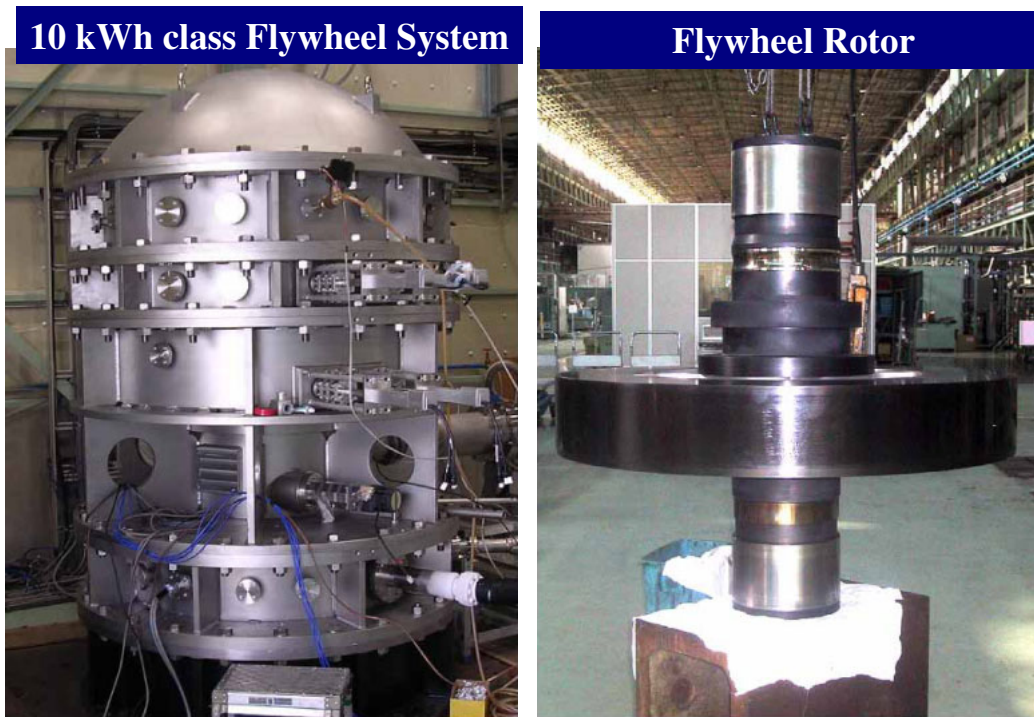


Fig. 18. (Color online) Cross section of HTS ramp-edge junction.



[Ishikawajima-Harima Heavy Industries Co., Ltd.]

Fig. 19. (Color online) Electricity storage system of flywheel type.

in width and 0.25 mm in thickness, and inside the sheath there are 55 filaments of Bi-2223 superconductor. Recently, Sumitomo has succeeded in producing higher-quality tapes by introducing a heat-treatment process under a high pressure of 300 atmospheric pressures, and has obtained a critical current of 200 A at 77 K.

9.2.2 Superconducting electric power cable

In 1998, Tokyo Electric Power Company and Sumitomo Electric Industries, Ltd. joined to produce a three-phase power transmission cable of 100 m, as shown in Fig. 21. Also Furukawa Electric Corp. made a single-phase transmission cable of 500 m in 2005.

9.2.3 Superconducting magnet for maglev trains

Our laboratory worked with the Central Railway Japan Corp. and Sumitomo Electric Industries, Ltd., to construct a magnet for a maglev train, using Bi-2223 superconducting tapes. The magnet has a racetrack shape and consists of twelve pancake coils, of 1 m length and 50 cm height, as shown in Fig. 22.

This magnet is operated at 20 K and generates a magnetic field of 2.5 T at the center of the magnet. Furthermore, the rate of decay of the persistent current is only 0.5% a day. This magnet is very successful and last October, a train using this magnet reached a speed of 500 km/h.

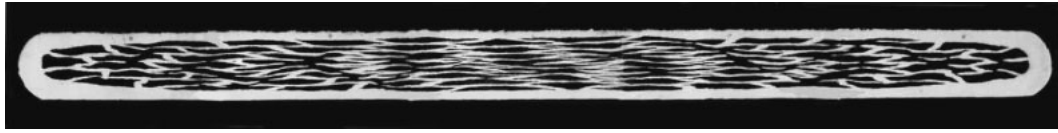


Fig. 20. Cross section of Ag sheathed Bi-2223 tape.

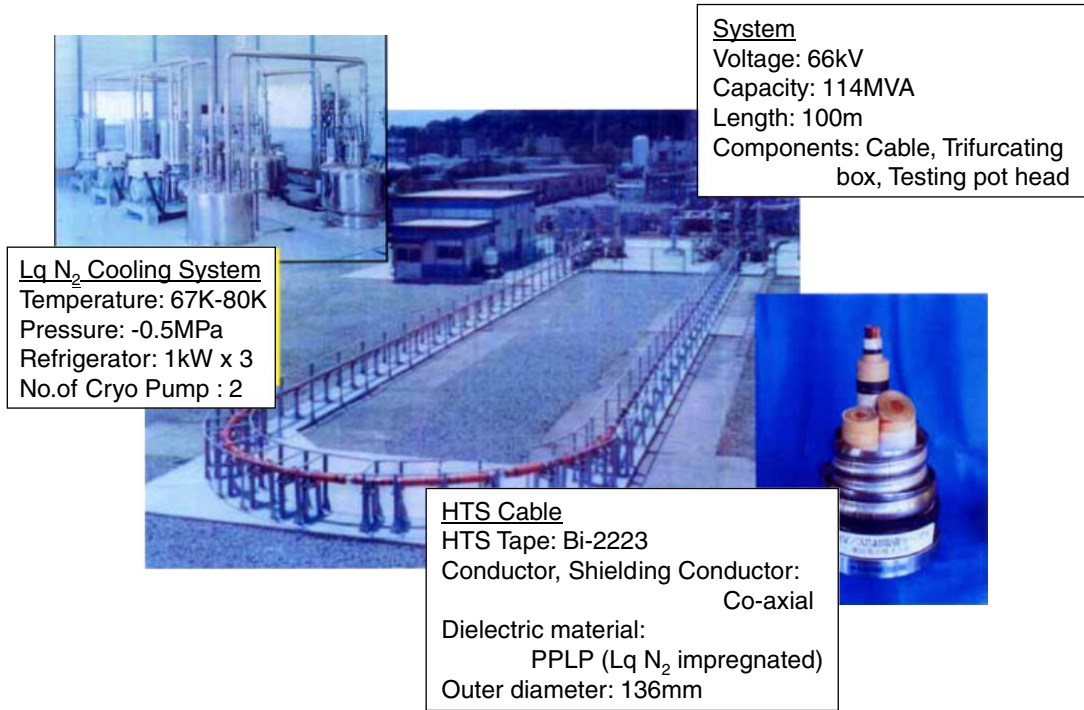


Fig. 21. (Color online) Field test of HTS cable.

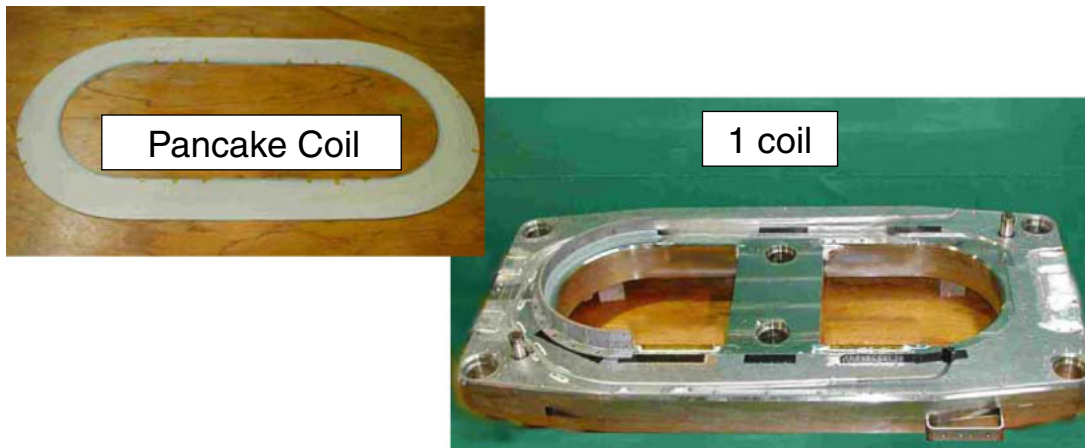


Fig. 22. (Color online) Development of racetrack-shaped coil manufacturing technology.

9.2.4 Development of next-generation superconducting tapes

Because silver-sheathed Bi-2223 tapes show a sharp decrease in critical current with increasing magnetic field at liquid-nitrogen temperature, superconducting tapes containing YBCO are under development to improve the magnetic field dependence.

The basic structure of YBCO tape consists of a thin metal plate, a buffer layer and a superconducting layer, as shown in Fig. 23.

The most difficult problem results from the fact that the

superconducting film consists of many small grains, and the critical current through the grain boundaries is very sensitive to the misfit angles between neighboring grains, as shown in Fig. 24.<sup>15)</sup> This sensitivity results from the d-wave symmetry of the superconductivity wave function.

To make the misfit angles as small as possible, the quality of the buffer layer (usually an oxide film) is important. This means that the misfit angles in the buffer layer must be very small. To obtain a high-quality buffer layer, a new method, ion-beam-assisted deposition (IBAD), has been developed by Fujikura, Ltd. in Japan. They chose GdZr<sub>2</sub>O<sub>7</sub> as a buffer

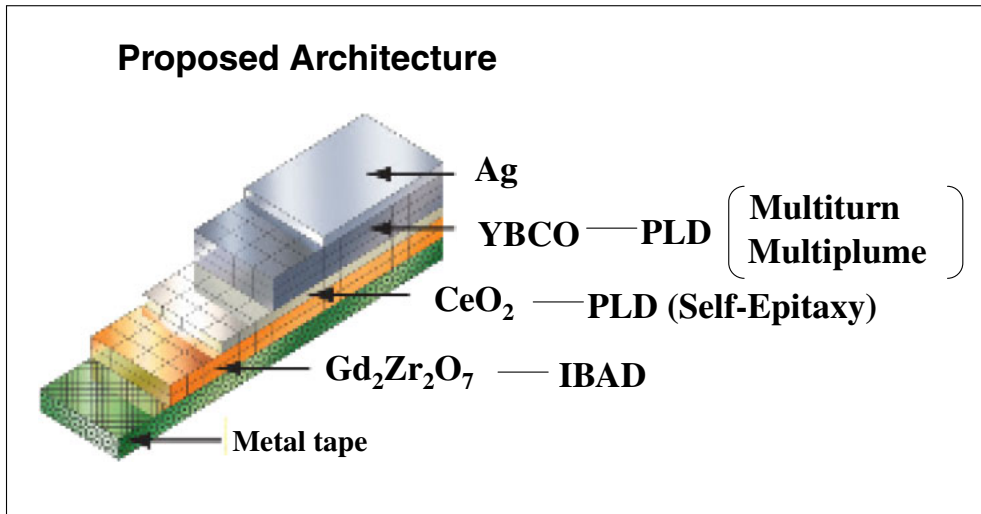


Fig. 23. (Color online) Structure of second-generation superconducting tape.

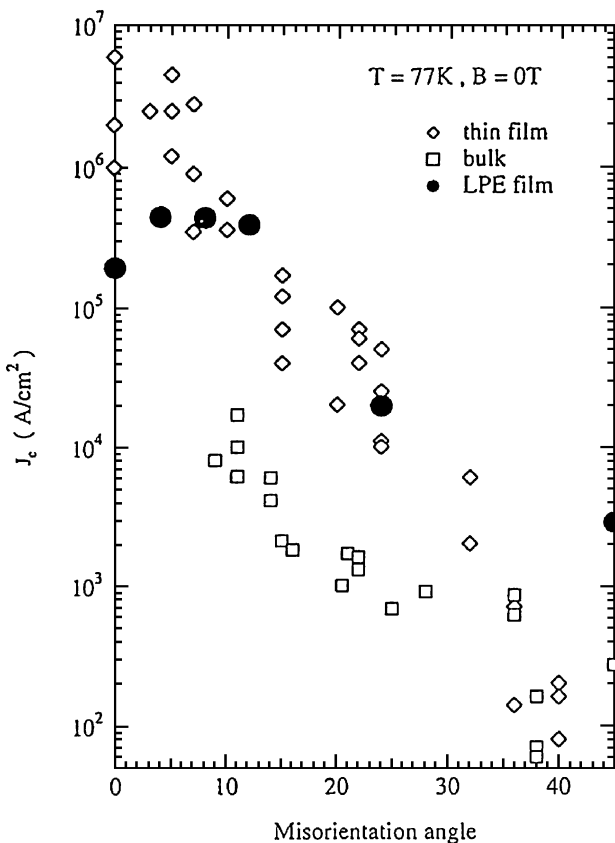


Fig. 24. Misorientation-angle dependence of critical current in YBCO bicrystals: (001)Kilt.

layer on hastelloy and obtained an average misfit angle of 10–15°. Then, we attached the thin  $CeO_2$  film as a cap layer, and found that the average misfit angle decreased to 4–5°. The dependence of the critical-current density of the YBCO film on the misfit angle is shown in Fig. 25, and then we obtained a high-quality YBCO tape, with a length of 250 m and a critical current of 250 A/cm at 77 K. At present, this is the highest value in the world (Fig. 26).

The low-temperature characteristics of this tape are very important. As shown in Fig. 27, the magnetic field depen-

dence is weak, and a critical-current density of more than  $10^5 A/m^2$  is obtained in a magnetic field of over 20 T at approximately 20 K. This indicates the capability of generating a magnetic field of over 20 T using a solenoid made of this type of superconducting tape at a low temperature. Therefore, the applications of next-generation tapes to high-resolution nuclear-magnetic-resonance systems, high-energy accelerators, and nuclear-fusion systems will become possible in future.

There are two other methods of preparing superconducting tape: one is metal organic deposition and the other is MOCVD. Both of them are under development at present, so they are not discussed in this report.

### 9.2.5 Superconducting motor for ships

The ship propulsion system is under going a revolution. In the new system, propellers and the electric motor are directly connected and they are outside the body of the ship, as shown in Fig. 28. By employing such a system, freedom of boat design is very much improved, and as a result, energy saving becomes possible. This propulsion system is called a “pod motor”, and a superconducting motor is the most suitable for this pod motor, because the superconducting motor generates a large torque even at a slow rotating propeller speed of about 100 rpm; furthermore, it is much smaller and much lighter than ordinary motors using copper wire.

In the United States, various types of superconducting motors are being developed, but all of them use Bi-2223 superconducting tape. In Japan, a superconducting motor using YBCO tape has been recently developed, and this is the first such motor in the world.

## 9.3 Superconducting electronic devices

### 9.3.1 Microwave filter

The simplest application of high-quality high-temperature superconducting film is the microwave filter. The high-quality thin film is fabricated on the plate of an MgO single crystal. The transmission characteristics of a well-designed filter are excellent, and in early stages of development it was hoped that many filtering systems would be used in the base

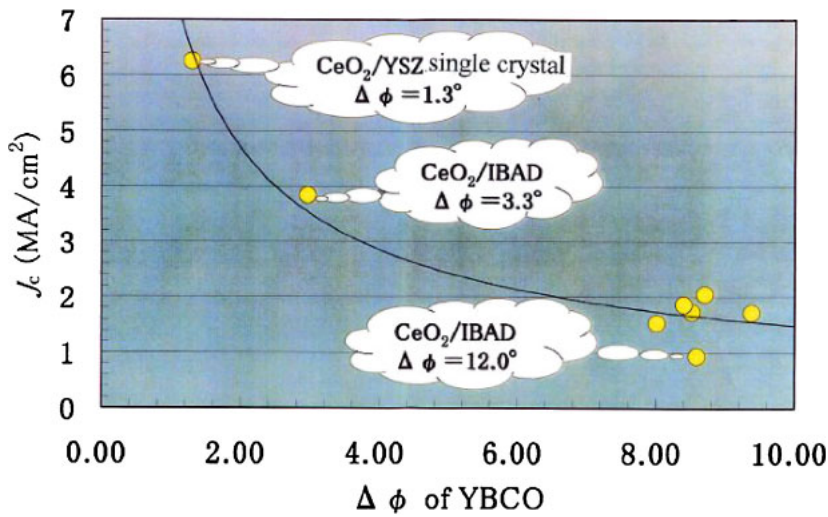
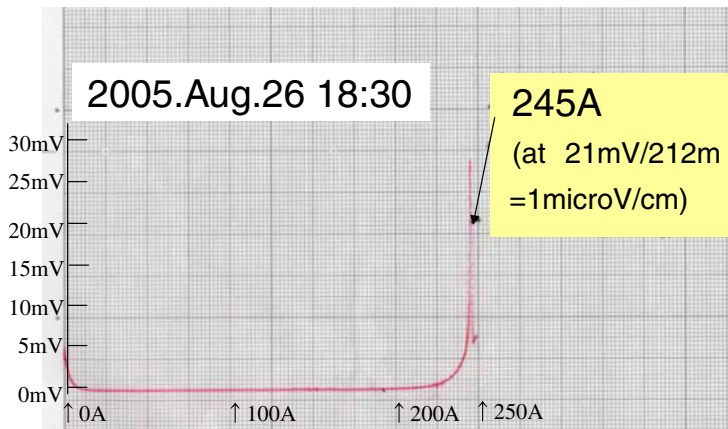
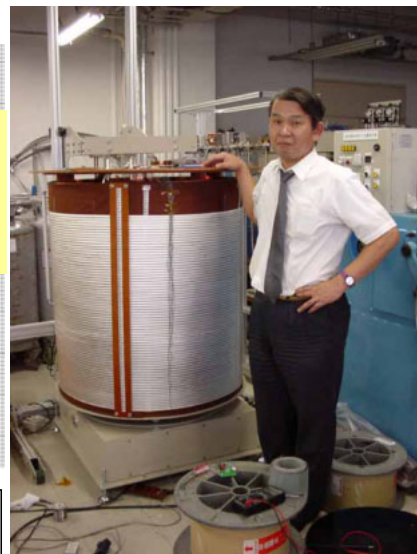


Fig. 25. (Color online) Relationship between YBCO/CeO<sub>2</sub>/IBAD  $\Delta\Phi$  and  $J_c$ .



**212.6 m x 245A=52087Am**

8 layers/30m/h = total production speed 3.75 m/h



Just after winding  
(95cm winding dia.)

Fig. 26. (Color online) Largest  $I_{cx}L$  Conductor (SRL Aug. 26, 2005).

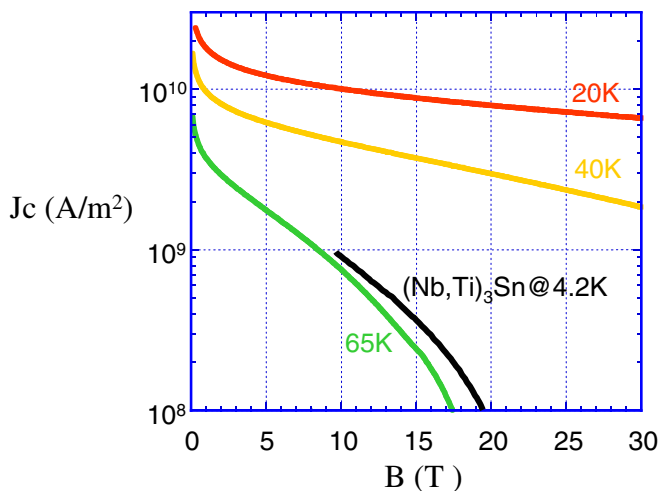


Fig. 27. (Color online) Comparison of  $J_c$ -B-T properties: YBCO, (Nb, Ti)<sub>3</sub>Sn.

stations of portable telephone systems. However, at present, only several thousand filters are employed in the world, because of the cost of the cooling system.

### 9.3.2 SQUID

The structure and characteristics of the SQUID system using a low-temperature Nb superconductor are well known. It shows very high sensitivity to a magnetic field.

In the case of using high temperature superconductors such as YBCO, the superconducting thin film is sputtered on the plate of a bicrystal, and Josephson junctions are formed on the crystal boundary. The sensitivity of SQUID systems using YBCO operating at 77 K is about ten times lower than that of an Nb-based system operating at 4 K, but by improving the manufacturing process and the design, the sensitivity will be increased in the near future.

Note that a SQUID system using a Hg-based high-temperature superconductor showed low flux noise level several times smaller than that using YBCO at 77 K.

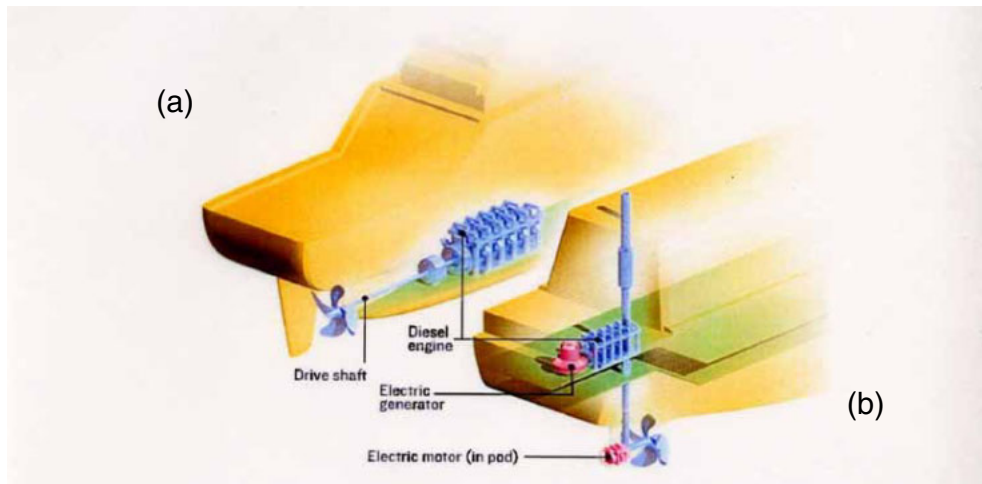


Fig. 28. (Color online) Comparison of propelling system; (a) ordinary system and (b) new system with pod motor.

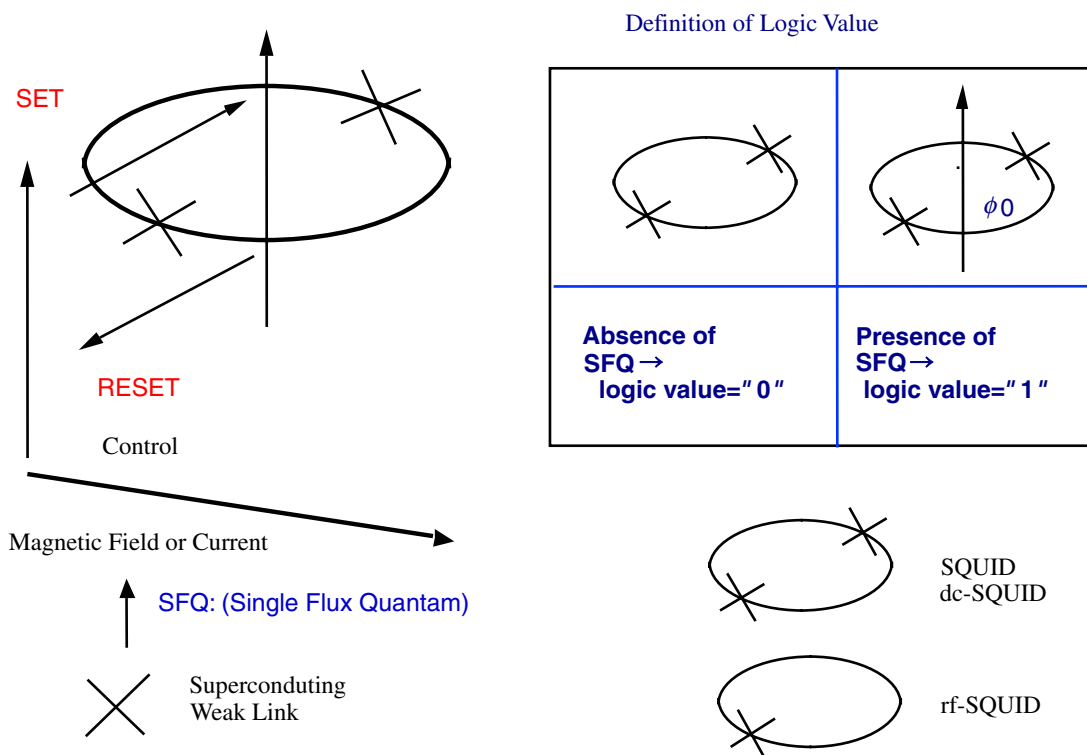


Fig. 29. (Color online) Controlling SFQ with use of SQUID.

The application of high-temperature SQUIDS to a magnetocardiograph has been made recently by Hitachi, Ltd.<sup>16)</sup> It consists of 51 SQUIDS on one plate and is used for the diagnosis of human heart diseases.

### 9.3.3 Single-quantum flux (SFQ) devices

The structure of a SFQ device is in principle the same as that shown in Fig. 29. In this superconductor ring, the magnetic field is quantized, and by applying a current pulse to the ring, the Josephson junction reaches a normal state for a short duration, and the quantized flux appears or disappears in the ring depending on the original state. The state of the flux in the ring is 0 or 1, and responds to the 0 or 1 of an information signal. Thus, this device acts as a flip-flop device. The transmission of quantized flux is performed using a Josephson transmission line, as shown in Fig. 30.

Combining these two devices, full logical operations can be performed.

The electricity consumption of the SFQ circuits is very small, 0.1 μW per one logic gate, and this is about one-hundredth that of semiconductor circuits. The operation speed is about 100 GHz, and this is one hundred times faster than that of semiconductor circuits.

In the past ten years, the circuit technology of SFQ circuits using Nb-based SFQs has made good progress, the integration of more than 10<sup>4</sup> junctions has become possible, and small-scale MPU, high-speed shift registers and high-speed switching systems have been developed.

Special features of SFQ circuits based on high-temperature superconductors are a high-speed operation of over 100 GHz and a high-temperature operation at approximately 40 K. On the other hand, the integration is more difficult than

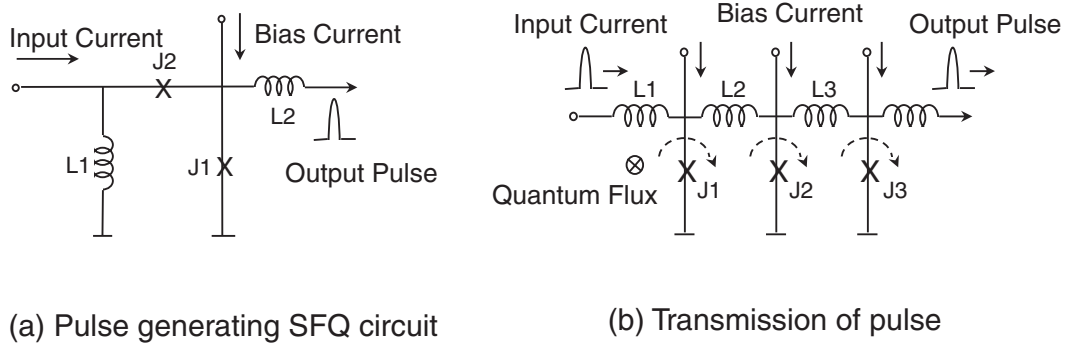


Fig. 30. Basic SFQ circuits.

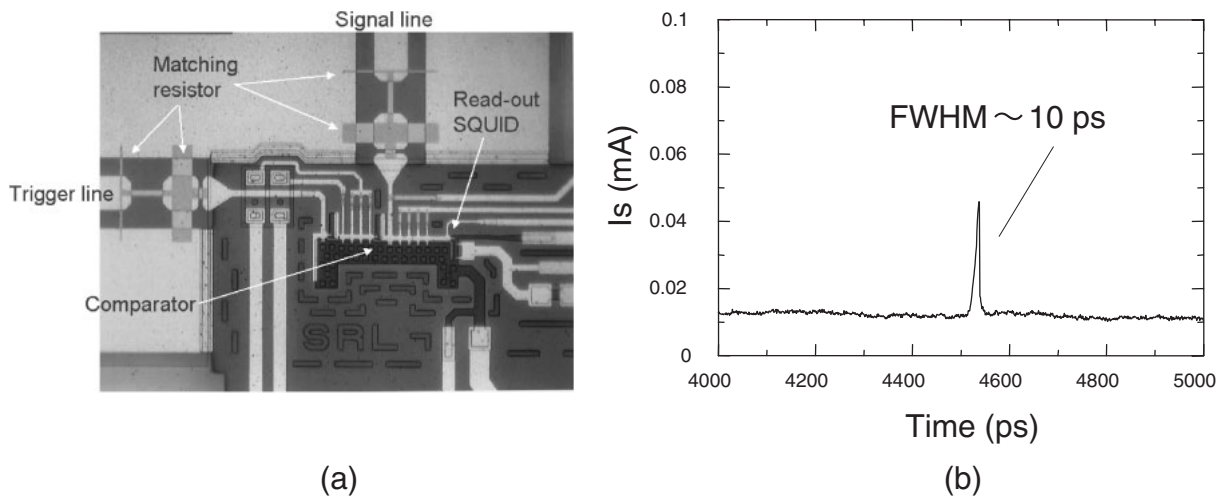


Fig. 31. (a) Photomicrograph of fabricated sampler chip including matching circuits. (b) Measured waveform of short-duration pulse generator.

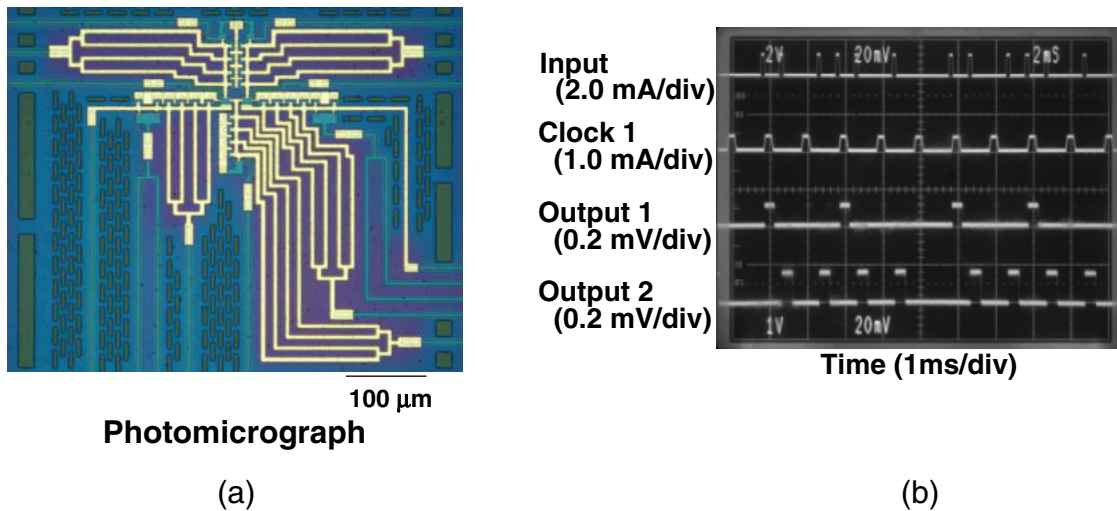


Fig. 32. (Color online) Fabricated 1:2 switch circuit.

that of Nb-based SFQ circuits owing to the complexity of process technology. In this report, two types of SFQ circuits are shown, one is a high-speed sampler and the other is a toggle flip-flop circuit. In both of them, about twenty Josephson junctions are used and operated at about 40 K.

The high-speed sampler is very useful for observing waveforms of a very short pulse greater than 40 GHz, which will be popular in future communication systems. Figure 31

is a photograph of the circuit of the sampler using YBCO junctions, and the obtained waveform of a high-speed pulse is also shown.<sup>17)</sup>

The toggle flip-flop circuit generates two output pulses for one input, and can be used as demultiplexer. Figure 32 shows a photograph of such a circuit, and the waveforms of one input and two output signals are shown for comparison. This circuit is operated faster than 370 GHz.<sup>18)</sup>

At present, the integration of a high-temperature SFQ circuit is limited to about 100 junctions, but it is hoped that this will reach to more than 500 junctions.

## 10. Summary

The discovery of high-temperature superconductivity is one of the most brilliant events in the 20th century, and it led to the wider physical concept of a “strongly correlated electron system”. This system is extremely complicated; thus, the physics of high-temperature superconductivity is not thoroughly understood yet. However, as far as the superconductivity problem, the classical concept of the Ginzburg-Landau theory can be applied qualitatively.

Before the discovery of high-temperature superconductivity, many excellent scientists tried to find this phenomenon for about 20 years, and we should not forget their endeavors. Thus, the author added a section on the prehistoric view in this report.

In the last ten years, many applications of high-temperature superconductivity have been made, and some of them are introduced in this report. These applications will spread to a very wide range of technologies, including information technology, and energy technology, and environmental technology. These are vital to the world in the 21st century.

The author hopes to accelerate the research and development of high-temperature superconductivity and its applications.

- 1) H. Frohlich: Proc. R. Soc. London, Ser. A **223** (1954) 296.
- 2) W. A. Little: Phys. Rev. A **134** (1964) 1416.
- 3) V. L. Ginzburg and D. A. Kirzhnits: *High-Temperature Superconductivity* (Consultant Bureau, 1977) [translated from Russian by A. K. Agyei].
- 4) C.-H. Hsu and M. M. Labes: J. Chem. Phys. **61** (1974) 4640.
- 5) A. W. Sleight, J. L. Gillson and F. E. Bielschmidt: Solid State Commun. **17** (1975) 27.
- 6) T. D. Tanh, A. Koma and S. Tanaka: Appl. Phys. **22** (1980) 205.

- 7) J. G. Bednorz and K. A. Muller: Z. Phys. B **64** (1986) 189.
- 8) H. Takagi, S. Uchida, K. Kitazawa and S. Tanaka: Jpn. J. Appl. Phys. **26** (1987) L123.
- 9) S. Tanaka: Jpn. J. Appl. Phys. **26** (1987) L203.
- 10) K. Kishio: J. Jpn. Inst. Met. **34** (1995) XXX.
- 11) K. Kishio, J. Shimoyama, T. Hasegawa, K. Kitazawa and K. Fueki: Jpn. J. Appl. Phys. **26** (1987) L1228.
- 12) T. Sekitani, Y. H. Matsuda, S. Ikeda, K. Uchida, F. Herlach, N. Miura, K. Nakao, T. Izumi, S. Tajima, M. Murakami, S. Hoshi, T. Koyama and Y. Shiohara: Physica C **392** (2003) 116.
- 13) M. Murakami: Prog. Mater. Sci. **38** (1994) 311.
- 14) K. Anagawa, Y. Yamada, T. Watanabe and M. Suzuki: IEEE Trans. Appl. Supercond. **15** (2005) 193.
- 15) D. Dimos, P. Chaudharia and J. Mannhart: Phys. Rev. B **41** (1990) 4038.
- 16) A. Tsukamoto, K. Saitoh, K. Yokosawa, D. Suzuki, Y. Seki, A. Kandori and K. Tsukada: IEEE Trans. Appl. Supercond. **15** (2005) 173.
- 17) H. Suzuki, T. Hato, M. Maruyama, H. Wakana, K. Nakayama, Y. Ishimaru, O. Horibe, S. Adachi, A. Kamitani, K. Suzuki, Y. Oshikubo, Y. Tarutani, K. Tanabe, T. Konno, K. Uekusa, N. Sato and H. Miyamoto: Physica C **426–431** (2005) 1643.
- 18) K. Tsubone, Y. Tarutani, H. Wakana, Y. Ishimaru, S. Adachi, K. Nakayama, Y. Oshikubo, O. Horibe, Y. Morimoto and K. Tanabe: Physica C **445–448** (2006) 1046.



**Shoji Tanaka** graduated from the Applied Mathematics Program, School of Technology, The University of Tokyo in 1950, and was appointed assistant professor at the School of Technology, The University of Tokyo in 1958, professor in 1968, and Professor Emeritus in 1988. He was appointed Vice President of the International Superconductivity Technology Center and Director General of Superconductivity Research Laboratory in 1988. He has achieved brilliant success in various research works including that on the semiconductor element structure, electron transport phenomenon, charge-density wave, and superconductivity. In 1999 he received the degree of Doctor of Science Honoris Causa from Purdue University in the U.S.A., and in 2005, he was engaged as Consultant Professor of Shanghai University.

He has received two awards from Japanese Emperor and some other international awards.